Journal of Statistical Modelling: Theory and Applications
pp. 1-23
Yazd University Press —

JSMTA

Research Paper

A Bayesian approach to process capability assessment for simple linear profiles

Zainab Abbasi Ganji*
Department of Statistics, Faculty of Mathematical Sciences, Ferdowsi University of Mashhad, Mashhad, Iran
Khorasan Razavi Agricultural and Natural Resources Research and Education Center, AREEO Mashhad, Iran

Received: August 25, 2025/ Revised: November 10, 2026/ Accepted: November 16, 2026

Abstract: In many industrial and manufacturing processes, product quality is characterised by a functional relationship between a response variable and an explanatory variable, commonly referred to as a simple linear profile. Assessing the capability of such profiles is a critical task in quality assurance, yet classical estimation methods provide only point estimates of capability indices and fail to quantify the associated uncertainty. To address this limitation, a Bayesian framework is proposed in this paper for estimating a recently developed profile capability index, which is obtained by averaging univariate capability indices across all levels of the explanatory variable. Non-informative priors are adopted for the model parameters, and a Gibbs sampling algorithm is employed to draw samples from the joint posterior distribution of the profile parameters, from which the posterior distribution of the capability index is derived. The performance of the proposed Bayesian estimator is compared with that of the classical ordinary least squares estimator through an extensive simulation study that considers multiple linear profile models, a range of sample sizes, and several error variances. The simulation results indicate that the Bayesian estimator performs better than its classical counterpart in most settings, with particularly substantial performance gains observed in small-sample scenarios, where the most pronounced reduction in estimation error is observed. Additionally, the Bayesian approach naturally provides credible intervals for the capability index, enabling a more comprehensive assessment of estimation uncertainty. The practical applicability of the proposed method is illustrated through a real-world manufacturing example.

Keywords: Bayesian inference; Credible interval; Gibs sampling; Process capability index; Simple linear profile.
Mathematics Subject Classification (2010): 62F15, 62P30, 62F25.

*Corresponding author: abbasiganji@alumni.um.ac.ir

Uncorrected Proof

1 Introduction

In contemporary industrial environments, the quality of manufactured products is frequently characterised not by a single measurable attribute, but by a functional relationship between a dependent variable and one or more independent variables. When this relationship can be adequately described by a simple linear regression model, it is referred to as a simple linear profile. Such profiles are encountered across a broad spectrum of applications, including sensor calibration, dose-response modelling, growth curve analysis, and quality monitoring in automated production systems. The accurate assessment of whether a process that generates such a profile is capable of meeting predefined engineering specifications is a fundamental task in quality engineering. However, unlike traditional univariate capability analysis, the functional nature of profile data introduces additional complexities, as variability must be evaluated simultaneously across the entire range of the explanatory variable, and the correlation structure among observations must be properly accounted for.

The literature on profile monitoring has grown considerably over the past two decades. Initial contributions in this area were primarily concerned with the detection of out-of-control conditions. For instance, Kang and Albin (2000) proposed a monitoring scheme based on a multivariate T^2 chart for the slope and intercept, combined with EWMA and R charts for residuals. Kim et al. (2003) suggested using three separate univariate control charts to monitor the intercept, slope, and error variance individually. Zou et al. (2006) developed a change-point model for detecting shifts in the parameters of a linear profile, while Woodall (2007) provided a comprehensive review of the early developments in this field. Noorossana et al. (2011) later offered a systematic treatment of profile monitoring techniques, covering both simple and more complex profile structures. Despite the richness of this body of work, the primary focus has consistently been on process surveillance and fault detection, rather than on capability assessment.

In contrast, the development of capability indices specifically designed for profiles has received comparatively less attention, despite its direct relevance to quality improvement and decision-making. Shahriari and Sarrafian (2009) proposed one of the earliest approaches, which was based on computing univariate C_{pk} indices at each level of the explanatory variable and then taking the minimum value as the overall capability measure. Hosseinifard and Abbasi (2012a,b) extended these ideas to accommodate both constant and functional specification limits, and also addressed the challenging case of non-normal profile data. Ebadi and Shahriari (2013) improved upon the earlier method by averaging the probabilities of nonconformance across different levels, rather than relying solely on the worst-case scenario. Wang (2014a,b) introduced yield-based indices that express capability in terms of the proportion of conforming product, while Wu (2015) developed a multivariate index that combines information from both the slope and the intercept into a single measure.

More recent advances have extended capability analysis to increasingly realistic and complex industrial settings. Pakzad et al. (2021) proposed functional capability indices that account for fuzziness in specification limits and measurements. In a follow-up study, Pakzad et al. (2022) introduced loss-based functional indices that incorporate economic penalties into the capability assessment. More recently, Pakzad et al. (2024) addressed the issue of within- and between-profile autocorrelation, which

Uncorrected Proof

is particularly relevant in processes where observations are collected sequentially over time. In the domain of fuzzy logic, Abbasi Ganji and Sadeghpour Gildeh (2020) developed fuzzy process capability indices for simple linear profiles, and Abbasi Ganji (2025) later extended the functional approach to fuzzy environments. Adibfar et al. (2023) investigated capability analysis for multivariate profiles, while Adibfar and Noorossana (2024) studied the more intricate case of multistage processes, where products undergo multiple sequential operations. Collectively, these developments underscore a growing consensus that capability assessment for profiles must be flexible enough to accommodate various sources of uncertainty, including fuzziness, autocorrelation, and the inherent complexity of modern manufacturing systems.

A notable limitation shared by many of the existing capability indices is their inability to adequately account for deviations from a target value, particularly when the specification limits are asymmetric. Moreover, most of these methods treat the different levels of the explanatory variable as equally important, even though the uncertainty associated with predictions and the proximity to specification limits may vary considerably across the range of the independent variable. To overcome these shortcomings, Abbasi Ganji and Sadeghpour Gildeh (2016) introduced a general class of capability indices, denoted by $C_p'''(u,v)$, which provides a unified framework that includes several classical indices as special cases. This class allows for flexible penalisation of both the deviation of the process mean from the target and the process variance, making it particularly well-suited for situations involving asymmetric tolerances. In a subsequent contribution, Abbasi Ganji and Sadeghpour Gildeh (2023) extended this class to the context of simple linear profiles and proposed an overall profile capability index, denoted by C'''_{ppM}. This index is obtained by averaging the estimated univariate indices across all levels of the explanatory variable, thereby providing a comprehensive summary of the capability of the entire profile.

Despite these advances, the existing formulation of C'''_{ppM} relies on classical estimation techniques. Such methods can be suboptimal when the sample size is limited or when the underlying distributional assumptions are violated. Specifically, the classical framework yields only a point estimate of the capability index and does not provide a direct mechanism for quantifying the accompanying uncertainty. This shortcoming is particularly critical in practical scenarios where decisions regarding process approval or corrective actions hinge on the reliability of the capability estimate. Moreover, the behavior of this index in small-sample regimes—which are frequently encountered in both industrial and clinical settings—has not yet been thoroughly investigated."

In this paper, we address these gaps by developing a Bayesian framework for estimating the process capability index C'''_{ppM} for simple linear profiles. The proposed approach offers several important advantages over the classical method. First, it provides not only a point estimate but also a full posterior distribution for the capability index, enabling the construction of credible intervals that directly quantify the uncertainty in the estimate. Second, by incorporating prior information through non-informative priors, the Bayesian method yields more stable and accurate estimates, particularly when the sample size is small. Third, the approach naturally handles the propagation of uncertainty from the estimated profile parameters to the final capability index, leading to more reliable inference. We employ Markov Chain Monte Carlo (MCMC) simulation using a Gibbs sampling algorithm to draw samples from the joint posterior

Uncorrected Proof

distribution of the profile parameters, and then compute the posterior distribution of the capability index by applying the definition of $\hat{C}'''_{ppM}$ to each sampled set of parameters.

A methodological contribution, rather than a merely computational one, is intended in this paper. To the best of our knowledge, no Bayesian estimator has previously been developed for the profile capability index C'''_{ppM}. The key step is the propagation of posterior uncertainty in the profile parameters through the nonlinear capability function, by which a full posterior distribution is obtained for the index instead of a single point estimate. It is this distributional output that permits a coherent probabilistic assessment of estimation uncertainty for the index, an assessment that is not available when the index is estimated by classical means.

The framework proposed here also differs from earlier Bayesian work on profiles. Previous Bayesian studies in this area have been largely directed at monitoring and at the detection of shifts in the profile parameters, or at capability assessment in univariate and simpler settings. In the present paper, inference is directed at the capability index of a simple linear profile itself, and the propagation of parameter uncertainty through the nonlinear capability function is treated as the central methodological problem.

A comprehensive simulation study is conducted to evaluate the performance of the proposed Bayesian estimator relative to the classical estimator under various process conditions. We consider three different linear profile models, multiple levels of error variance, and a range of sample sizes, including small samples where the benefits of the Bayesian approach are expected to be most pronounced. The results demonstrate that the Bayesian estimator outperforms its classical counterpart in the majority of settings, with the most notable advantages appearing when sample sizes are limited. Furthermore, we show that the credible intervals obtained from the Bayesian approach exhibit excellent coverage properties, achieving levels close to the nominal 95% across all settings.

The remainder of this paper is organized as follows. Section 2 reviews the class $C'''_p(u, v)$ and its extension to simple linear profiles, including the definition of the overall index $\hat{C}'''_{ppM}$. Section 3 describes the proposed Bayesian estimation procedure, detailing the prior specifications, the MCMC algorithm, and the computational implementation. Section 4 presents the simulation design and the results of the comparative study. Section 5 illustrates the practical applicability of the proposed method through a real-world manufacturing example. Finally, Section 6 concludes the paper and discusses potential directions for future research.

2 Preliminaries

In this section, we briefly review the essential concepts required for the development of the proposed Bayesian estimation procedure. We begin by defining the simple linear profile model and describing the standard estimation approach based on ordinary least squares (OLS). We then introduce the class of capability indices from which our profile index is derived, and finally define the overall capability index for the entire profile.

Uncorrected Proof

2.1 Profile model and estimation

Consider a process in which the quality characteristic of interest is characterized by a simple linear relationship between a response variable Y and an explanatory variable X. Suppose that data are collected at k fixed levels of the explanatory variable, denoted by $x_1, x_2, \ldots, x_k$, and that at each level, n independent observations are available. For the j-th sample, the observed response at the i-th level is denoted by Y_{ij}. When the process is in a state of statistical control, the relationship is assumed to follow the linear model

$$Y_{ij} = A_0 + A_1 X_i + \varepsilon_{ij}, \quad i = 1, 2, \ldots, k, \quad j = 1, 2, \ldots, n, \tag{1}$$

where A_0 and A_1 are the intercept and slope parameters, respectively, and the error terms ε_{ij} are independently and identically distributed as normal random variables with mean zero and constant variance σ^2.

The parameters of the profile are typically estimated using ordinary least squares. For the j-th sample, the least squares estimates of the slope and intercept are given by

$$a_{1j} = \frac{S_{xy(j)}}{S_{xx}}, \qquad a_{0j} = \bar{y}_j - a_{1j}\bar{x},$$

where $\bar{y}_j = \frac{1}{k}\sum_{i=1}^{k} y_{ij}$, $\bar{x} = \frac{1}{k}\sum_{i=1}^{k} x_i$, $S_{xy(j)} = \sum_{i=1}^{k}(x_i - \bar{x})y_{ij}$, and $S_{xx} = \sum_{i=1}^{k}(x_i - \bar{x})^2$. To obtain overall estimates of the profile coefficients across all samples, we average the sample-specific estimates:

$$\hat{A}_0 = a_0 = \frac{1}{n}\sum_{j=1}^{n} a_{0j}, \qquad \hat{A}_1 = a_1 = \frac{1}{n}\sum_{j=1}^{n} a_{1j}.$$

The error variance is estimated by the pooled mean squared error, defined as $\hat{\sigma}^2 = \mathrm{MSE} = \frac{1}{n}\sum_{j=1}^{n} \mathrm{MSE}_j$, where $\mathrm{MSE}_j = \frac{\sum_{i=1}^{k}(y_{ij} - \hat{y}_{ij})^2}{k-2}$, and $\hat{y}_{ij} = a_{0j} + a_{1j}x_i$ is the fitted value for the j-th sample at the i-th level. The predicted response at level x_i, based on the overall estimates, is denoted by $\hat{Y}_i = a_0 + a_1 x_i$. Since a_0 and a_1 are obtained by averaging the n independent sample-specific OLS estimates, the variance of $\hat{Y}_i$, conditional on the fixed design level x_i, is given by

$$\mathrm{Var}(\hat{Y}_i) = \sigma^2 \left(\frac{1}{nk} + \frac{(x_i - \bar{x})^2}{nS_{xx}} \right). \tag{2}$$

Equation (2) is obtained in three steps. First, for a single sample j, the variance of the OLS prediction at level x_i is

$$\mathrm{Var}(\hat{Y}_{ij} \mid x_i) = \sigma^2 \left(\frac{1}{k} + \frac{(x_i - \bar{x})^2}{S_{xx}} \right).$$

Second, because the overall estimate $\hat{Y}_i$ is the average of the n independent sample-specific predictions, its variance is obtained by dividing the above expression by n, which gives

$$\mathrm{Var}(\hat{Y}_i \mid x_i) = \frac{\sigma^2}{n} \left(\frac{1}{k} + \frac{(x_i - \bar{x})^2}{S_{xx}} \right) = \sigma^2 \left(\frac{1}{nk} + \frac{(x_i - \bar{x})^2}{nS_{xx}} \right).$$

Uncorrected Proof

Finally, the unknown variance σ^2 is replaced by its unbiased estimator MSE, which yields Equation (2). In this expression, the term $1/(nk)$ reflects the uncertainty associated with the estimated intercept, whereas the term $(x_i - \bar{x})^2/(nS_{xx})$ reflects the additional uncertainty introduced by the estimated slope at points away from the center of the design. It should be noted that Equation (2) gives the variance of the fitted mean response at level x_i, and not the variance of a future observation at that level.

This expression reflects both the sampling variability and the uncertainty arising from the position of x_i relative to the centre of the design space.

2.2 Capability index for profiles

To assess the capability of a simple linear profile, we adopt the general class of capability indices proposed by Abbasi Ganji and Sadeghpour Gildeh (2016). This class, denoted by $C_p'''(u, v)$, is defined as

$$C_p'''(u, v) = \frac{d^* - uA^*}{3\sqrt{\sigma^2 + vA^2}}, \quad u, v \geq 0,$$

where $d^* = \min\{D_l, D_u\}$ is the minimum distance from the target value T to the specification limits, with $D_l = T - \text{LSL}$ and $D_u = \text{USL} - T$. The quantities A^* and A^2 penalise deviations of the process mean μ from the target T, and are defined as

$$A^* = \frac{(\mu - T)^2}{D_u} I\{\mu > T\} + \frac{(T - \mu)^2}{D_l} I\{\mu \leq T\}, \tag{3}$$

$$A^2 = \frac{d^2(\mu - T)^2}{D_u^2} I\{\mu > T\} + \frac{d^2(T - \mu)^2}{D_l^2} I\{\mu \leq T\}, \tag{4}$$

with $d = (\text{USL} - \text{LSL})/2$, and $I\{\cdot\}$ denoting the indicator function. The tuning parameters u and v control the degree of penalisation applied to the deviation from the target and the process variance, respectively. This formulation provides a unified framework that encompasses several classical capability indices as special cases.

For application to simple linear profiles, the above univariate formulation must be adapted to account for the functional nature of the data. At a given level x_i of the explanatory variable, the estimated index is obtained by replacing the process mean μ with the predicted response $\hat{Y}_i$, the process variance σ^2 with the prediction variance, and the specification limits with their corresponding values at that level.

For capability assessment, however, the specification limits are attached to individual measurements rather than to the fitted mean response. The appropriate quantity for the denominator of the index is therefore the variance of the difference between a future observation and the fitted mean, rather than the variance of the fitted mean alone. This prediction variance is obtained by adding the variance of the new observation, σ^2, to the variance of the fitted mean given in (2), which yields

$$\text{Var}(Y_{\text{new},i} - \hat{Y}_i) = \sigma^2 + \sigma^2 \left[\frac{1}{nk} + \frac{(x_i - \bar{x})^2}{nS_{xx}}\right] = \sigma^2 \left[1 + \frac{1}{nk} + \frac{(x_i - \bar{x})^2}{nS_{xx}}\right].$$

Replacing the unknown variance σ^2 by its unbiased estimator MSE gives the estimated

Uncorrected Proof

prediction variance

$$\widehat{\mathrm{Var}}(Y_{\mathrm{new},i} - \hat{Y}_i) = \mathrm{MSE}\left[1 + \frac{1}{nk} + \frac{(x_i - \bar{x})^2}{nS_{xx}}\right],$$

which is the quantity that enters the local capability index defined below. Specifically, the estimated local index at the i-th level is given by

$$\hat{C}'''_{pi}(u,v) = \frac{\hat{d}_i^* - u\hat{A}_i^*}{3\sqrt{\mathrm{MSE}\left(1 + \frac{1}{nk} + \frac{(x_i-\bar{x})^2}{nS_{xx}}\right) + v\hat{A}_i^2}},$$

where $\hat{d}_i^* = \min\{\hat{D}_{li}, \hat{D}_{ui}\}$, with $\hat{D}_{li} = \hat{Y}_i - \mathrm{LSL}_i$, $\hat{D}_{ui} = \mathrm{USL}_i - \hat{Y}_i$, and $\hat{A}_i^*$ and $\hat{A}_i^2$ are defined analogously to (3) and (4), with μ replaced by $\hat{Y}_i$, and D_l, D_u, d replaced by their level-specific counterparts. The inclusion of the prediction variance in the denominator ensures that the uncertainty associated with the estimated profile coefficients is properly propagated into the capability assessment.

To obtain a single overall measure of capability for the entire profile, we average the local indices across all k levels of the explanatory variable:

$$\hat{C}'''_{pM}(u,v) = \frac{1}{k}\sum_{i=1}^{k} \hat{C}'''_{pi}(u,v).$$

This overall index summarizes the capability of the process across the full range of the explanatory variable, taking into account both the variability at each level and the uncertainty in the estimated profile.

In the original formulation of Abbasi Ganji and Sadeghpour Gildeh (2023), the index $\hat{C}'''_{ppM}$ was introduced with the specific choice of $u = v = 1$. This baseline selection ensures a balanced penalization of both the deviation from the target and the process variance. In the present paper, we adopt this same formulation—that is, we fix $u = v = 1$—and focus on developing a Bayesian approach for estimating the resulting index, rather than on selecting or optimizing the tuning parameters. The Bayesian framework provides a natural way to account for parameter uncertainty and to construct credible intervals for the capability index, which are not readily available under the classical estimation approach. In the following section, we describe the proposed Bayesian estimation procedure in detail.

3 Bayesian estimation procedure

In this section, the proposed Bayesian framework for estimating the profile capability index C'''_{ppM} is described in detail. The aim is to provide a comprehensive account of the modelling assumptions, prior specifications, computational algorithm, and the manner in which the posterior distribution of the capability index is obtained. The exposition is organized such that each component of the estimation procedure is presented in a logical sequence, beginning with the likelihood function and culminating in the construction of credible intervals for the index.

Uncorrected Proof

3.1 Model specification and likelihood function

Recall from Section 2 that, for a simple linear profile, the observed response at the i-th level of the explanatory variable and the j-th sample is modelled as

$$Y_{ij} = A_0 + A_1 x_i + \varepsilon_{ij}, \quad i = 1, 2, \ldots, k, \quad j = 1, 2, \ldots, n,$$

where the errors ε_{ij} are assumed to be independently and normally distributed with mean zero and variance σ^2. Under this assumption, the likelihood function for the observed data $\mathbf{Y} = \{Y_{ij} : i = 1, \ldots, k; j = 1, \ldots, n\}$, conditional on the unknown parameters A_0, A_1, and σ^2, is given by

$$p(\mathbf{Y} \mid A_0, A_1, \sigma^2) \propto (\sigma^2)^{-nk/2} \exp\left\{ -\frac{1}{2\sigma^2} \sum_{j=1}^{n} \sum_{i=1}^{k} (Y_{ij} - A_0 - A_1 x_i)^2 \right\}.$$

This likelihood function forms the basis for the Bayesian inference, as it summarizes the information about the parameters contained in the data.

3.2 Prior distributions

In the Bayesian paradigm, prior distributions must be specified for all unknown parameters. Since the primary objective of this study is to develop an objective and data-driven estimation procedure, non-informative priors are adopted. This choice ensures that the posterior inference is dominated by the observed data, and that any subjective influence from the prior is minimized.

Specifically, the following prior structure is employed:

• For the regression coefficients A_0 and A_1, a flat (improper uniform) prior is assumed, i.e., $p(A_0, A_1) \propto 1$. This expresses the state of complete ignorance about the plausible values of the intercept and slope, allowing the data to determine their estimates freely.

• For the error variance σ^2, the Jeffreys prior is used, which is given by $p(\sigma^2) \propto 1/\sigma^2$. This prior is invariant under reparameterization and is a standard choice for variance parameters in normal models when no prior information is available. It is worth noting that this prior is equivalent to an inverse-gamma distribution with shape and scale parameters approaching zero, i.e., $\sigma^2 \sim \text{Inv-Gamma}(\epsilon, \epsilon)$ with $\epsilon \to 0$.

The joint prior distribution for all parameters is therefore

$$p(A_0, A_1, \sigma^2) \propto \frac{1}{\sigma^2}.$$

This prior structure is intentionally chosen to be as non-informative as possible, so that the resulting posterior distribution reflects only the information provided by the data. A sensitivity analysis to alternative proper and weakly informative prior specifications is reported in Section 4.5.

3.3 Joint posterior distribution and Gibbs sampling

By Bayes' theorem, the joint posterior distribution of the parameters is proportional to the product of the likelihood and the prior:

$$p(A_0, A_1, \sigma^2 \mid \mathbf{Y}) \propto p(\mathbf{Y} \mid A_0, A_1, \sigma^2) \times p(A_0, A_1, \sigma^2).$$

Uncorrected Proof

Under the prior specifications described above, the full conditional distributions of the parameters take simple and standard forms, which makes the implementation of a Gibbs sampling algorithm straightforward. The Gibbs sampler is a MCMC method that iteratively samples each parameter from its full conditional distribution, conditional on the current values of the other parameters.

The full conditional distributions required for the Gibbs sampler are derived as follows:

1. **Conditional distribution of σ^2:** Given the data and the current values of A_0 and A_1, the conditional posterior distribution of σ^2 is an inverse-gamma distribution:

$$\sigma^2 \mid \mathbf{Y}, A_0, A_1 \sim \text{Inv-Gamma}\left(\frac{nk}{2}, \frac{1}{2}\sum_{j=1}^{n}\sum_{i=1}^{k}(Y_{ij} - A_0 - A_1 x_i)^2\right). \tag{5}$$

2. **Conditional distribution of (A_0, A_1):** Given the data and σ^2, the joint conditional posterior distribution of the regression coefficients is multivariate normal:

$$\begin{pmatrix} A_0 \\ A_1 \end{pmatrix} \mid \mathbf{Y}, \sigma^2 \sim \mathcal{N}_2\left(\hat{\boldsymbol{\beta}}, \sigma^2(\mathbf{X}^\top\mathbf{X})^{-1}\right), \tag{6}$$

where $\hat{\boldsymbol{\beta}} = (\hat{A}_0, \hat{A}_1)^\top$ is the ordinary least squares estimate of the coefficient vector, and $\mathbf{X}$ is the $(nk) \times 2$ design matrix with rows $(1, x_i)$.

The Gibbs sampler proceeds by iteratively drawing samples from these two conditional distributions. Starting from an initial value (which can be taken as the OLS estimates), the algorithm cycles through the following steps:

- Sample σ^2 from its inverse-gamma conditional distribution in 5.
- Sample A_0 and A_1 jointly from their multivariate normal conditional distribution in 6.

After a sufficiently large number of iterations, the generated samples converge to the target joint posterior distribution. The first M iterations are discarded as a burn-in period to allow the chain to reach its stationary distribution. The remaining samples are then used for posterior inference.

3.4 Posterior distribution of the capability index

Once a set of posterior samples for the profile parameters has been obtained, the next step is to compute the corresponding samples of the capability index. For each retained MCMC draw $t = 1, 2, \ldots, T$, the following procedure is applied:

1. Using the sampled parameter values $A_0^{(t)}$, $A_1^{(t)}$, and $\sigma^{2(t)}$, the predicted response at each level x_i is computed as

$$\hat{Y}_i^{(t)} = A_0^{(t)} + A_1^{(t)} x_i, \quad i = 1, 2, \ldots, k.$$

2. For each level x_i, the local capability index $\hat{C}_{ppi}^{\prime\prime\prime(t)}$ is computed with $A_0^{(t)}$, $A_1^{(t)}$, and $\sigma^{2(t)}$ in place of their OLS counterparts.

3. The local indices are then averaged across the k levels to obtain the overall profile capability index for the t-th draw: $\hat{C}_{ppM}^{\prime\prime\prime(t)} = \frac{1}{k}\sum_{i=1}^{k}\hat{C}_{ppi}^{\prime\prime\prime(t)}$.

Uncorrected Proof

After performing this calculation for all T retained draws, the resulting collection $\{\hat{C}_{ppM}^{\prime\prime\prime(t)} : t = 1, \ldots, T\}$ constitutes an empirical approximation to the posterior distribution of the capability index. This posterior sample can then be summarized in various ways:

• **Point estimate:** The posterior mean of the capability index is taken as the Bayesian point estimate, i.e., $\widehat{BC}_{ppM}^{\prime\prime\prime} = \frac{1}{T}\sum_{t=1}^{T} \hat{C}_{ppM}^{\prime\prime\prime(t)}$.

• **Credible interval:** A $100(1-\alpha)\%$ credible interval for the true capability index is obtained by computing the $\alpha/2$ and $1-\alpha/2$ quantiles of the posterior sample. Formally, if $\hat{C}_{ppM}^{\prime\prime\prime(1)}, \hat{C}_{ppM}^{\prime\prime\prime(2)}, \ldots, \hat{C}_{ppM}^{\prime\prime\prime(T)}$ denote the T retained draws from the posterior distribution of the capability index, then the lower and upper bounds of the credible interval are given by $\left(C_{ppM}^{\prime\prime\prime(\alpha/2)},\ C_{ppM}^{\prime\prime\prime(1-\alpha/2)}\right)$, where $\hat{C}_{ppM}^{\prime\prime\prime(\alpha/2)}$ and $\hat{C}_{ppM}^{\prime\prime\prime(1-\alpha/2)}$ are the $\alpha/2$-th and $(1-\alpha/2)$-th empirical quantiles of the posterior sample. This interval has a direct probabilistic interpretation: given the observed data and the assumed prior distributions, the probability that the true capability index lies within this interval is exactly $1-\alpha$. This is in contrast to the classical confidence interval, which does not have such a direct interpretation and is often misunderstood in practice. The ability to construct such intervals is one of the key advantages of the Bayesian framework, as it provides quality engineers with a coherent and intuitive measure of estimation uncertainty.

• **Uncertainty assessment:** The standard deviation of the posterior sample can be used as a measure of estimation uncertainty, which is analogous to the standard error in the classical framework but does not rely on asymptotic approximations.

3.5 Implementation and convergence diagnostics

The Gibbs sampling algorithm was implemented in the R statistical computing environment, available in R Core Team (2024). For each simulated dataset, four parallel chains were initiated from dispersed starting values, and each chain was run for 3000 iterations. The first 1500 iterations of every chain were discarded as burn-in, and the remaining 1500 draws were retained for posterior inference. To guarantee reproducibility, a fixed random seed was established prior to the analysis.

Convergence was monitored through three standard diagnostics: visual inspection of trace plots, the Gelman-Rubin statistic $\hat{R}$, introduced by Gelman and Rubin (1992), and the effective sample size (ESS). The trace plots corresponding to a representative setting (Model 1, $n = 20$, $\sigma = 0.5$) are displayed in Figure 1. It is evident from the three panels that the chains overlap and oscillate around stable values without any systematic trends or long excursions. Such behavior confirms that the chains have reached their stationary distribution and are well mixed.

The corresponding numerical diagnostics for this setting are summarized in Table 1. To ensure that these results are not specific to a single scenario, the same diagnostics were computed for all 27 simulation settings. Across the entire study, the maximum value of $\hat{R}$ was found to be 1.0114, and the minimum effective sample size was 1561. Both values are well within the conventional thresholds of 1.05 and 400, respectively, as recommended by Gelman et al. (1995). These results collectively demonstrate that satisfactory convergence was achieved throughout the simulation study and that the posterior estimates reported in this paper are based on a sufficient number of effectively independent draws.

Uncorrected Proof

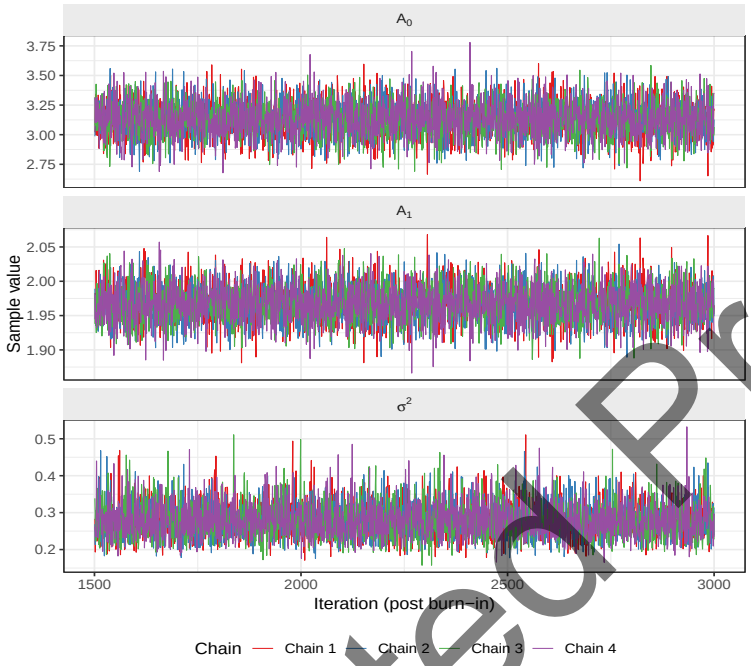

Figure 1: Trace plots for A_0, A_1, and σ^2 in a representative seting (Model 1, $n = 20$, $\sigma = 0.5$).

Table 1: Convergence diagnostics for the representative simulation setting (Model 1, $n = 20$, $\sigma = 0.5$).

Parameter	$\hat{R}$	Upper 95% bound of $\hat{R}$	ESS
A_0	1.0004	1.0009	6000
A_1	1.0007	1.0019	6000
σ^2	0.9999	1.0003	5553

The computational burden of the Gibbs sampler was modest. Because closed-form conditional distributions were available, rapid sampling was achieved without the need for tuning or adaptive steps. For a dataset with $n = 20$ and $k = 4$, each chain was completed in less than one second on a standard desktop computer, which makes the procedure computationally feasible for routine quality engineering applications.

All computations were performed using the `MASS` package for multivariate normal sampling and the `coda` package developed by Plummer et al. (2006) for diagnostic evaluation. The R code used to generate the simulation results and the convergence diagnostics is available from the corresponding author upon request.

3.6 Summary of the Bayesian procedure

For ease of reference, the main steps of the proposed Bayesian estimation procedure are summarized below:

1. Collect the profile data $\{Y_{ij} : i = 1, \ldots, k; j = 1, \ldots, n\}$ and fix the specification

Uncorrected Proof

limits (LSL_i, USL_i) and target values T_i for each level of the explanatory variable.
2. Specify the model as in (1) and assign the non-informative priors $p(A_0, A_1) \propto 1$ and $p(\sigma^2) \propto 1/\sigma^2$.
3. Run the Gibbs sampling algorithm to obtain T retained draws from the joint posterior distribution of the profile parameters (A_0, A_1, σ^2).
4. For each retained draw, compute the corresponding value of the capability index $\hat{C}'''^{(t)}_{ppM}$ using the averaging procedure described in Section 3.4.
5. Use the posterior sample of the index to compute the Bayesian point estimate (posterior mean), credible intervals, and any other summary measures of interest.

This procedure yields a comprehensive and probabilistically coherent assessment of the process capability, with the additional benefit of quantifying the uncertainty associated with the index estimate

4 Simulation study

In this section, we present a comprehensive simulation study designed to evaluate the performance of the proposed capability index $\widehat{BC}'''_{ppM}$ in the context of simple linear profiles. The primary objectives of this simulation study are threefold: (i) to compare the bias and mean squared error (MSE) of the Bayesian estimator with those of the classical OLS estimator, (ii) to assess the effect of sample size and error variance on the estimation accuracy, and (iii) to examine the behavior of the Bayesian estimator across different profile models.

4.1 Simulation design

The simulation study is based on the framework introduced by Kang and Albin (2000), which has been widely used in the profile monitoring literature. We consider three simple linear profile models, each defined by different values of the intercept and slope parameters. The models are

$$\begin{aligned} &\text{Model 1:} && Y_{ij} = 3.0 + 2.0\, x_i + \varepsilon_{ij}, \\ &\text{Model 2:} && Y_{ij} = 3.5 + 2.0\, x_i + \varepsilon_{ij}, \\ &\text{Model 3:} && Y_{ij} = 3.4 + 2.4\, x_i + \varepsilon_{ij}. \end{aligned}$$

For each model, the explanatory variable x is fixed at four levels, namely $x = 2, 4, 6$, and 8, which are the same design points used in the original study by Kang and Albin (2000). The error terms ε_{ij} are generated independently from a normal distribution with mean zero and variance σ^2. Three levels of error variance are considered: $\sigma = 0.5, 0.8$, and 1.0, representing low, moderate, and high noise conditions, respectively.

For each combination of model, error variance, and sample size, we generate $N_{\text{sim}} = 500$ independent datasets. In each dataset, a total of n independent samples are collected, where each sample consists of $k = 4$ observations corresponding to the four levels of x. Three sample sizes are considered: $n = 20, 50$, and 100, covering small, moderate, and large sample scenarios. This results in a total of 3 models $\times$ 3 error variances $\times$ 3 sample sizes = 27 simulation settings.

Uncorrected Proof

For each generated dataset, we compute the index $\hat{C}'''_{ppM}$ using both the classical OLS method and the proposed Bayesian approach. In the classical method, the profile parameters are estimated using the standard least squares formulas, and the index is computed directly from these estimates. In the Bayesian method, we use a Gibbs sampling algorithm to draw samples from the joint posterior distribution of the profile parameters, and then obtain the posterior distribution of the capability index. The Bayesian point estimate is taken as the posterior mean.

The specification limits and target values used in the computation of the capability index are reproduced in Table 2 for completeness. These limits are defined at each level of the explanatory variable.

Table 2: Specification limits and target values for each level of the explanatory variable.

x_i	2	4	6	8
LSL	2.50	6.25	10.60	14.35
USL	10.60	14.35	18.75	23.75
Target	6.25	10.60	14.35	18.75

4.2 Evaluation criteria

To compare the performance of the classical and Bayesian estimators, we use two standard criteria: bias and mean squared error (MSE). For a given simulation setting, let $\hat{C}^{(t)}$ denote the estimated capability index from the t-th replication, and let C denote the true value of the capability index computed from the true model parameters. Then, the bias and MSE are defined as

$$\text{Bias} = \frac{1}{N_{\text{sim}}} \sum_{t=1}^{N_{\text{sim}}} \left(\hat{C}^{(t)} - C \right),$$

$$\text{MSE} = \frac{1}{N_{\text{sim}}} \sum_{t=1}^{N_{\text{sim}}} \left(\hat{C}^{(t)} - C \right)^2.$$

A smaller absolute bias indicates that the estimator is more accurate on average, while a smaller MSE indicates that the estimator is more precise and has lower overall error.

4.3 Simulation results

The results of the simulation study are summarized in Table 3, which presents the bias and MSE for both the classical and Bayesian estimators under each of the 27 simulation settings.

The results reveal several important patterns:

1. The Bayesian estimator outperforms the classical estimator in terms of MSE in the vast majority of settings. Specifically, in 24 out of 27 simulation settings (88.9%), the Bayesian method yields a smaller MSE than the classical method. This advantage is particularly pronounced for Model 1 and Model 2, where the Bayesian estimator achieves MSE reductions ranging from approximately 33% to 58%. For Model 3, the performance gains are generally less substantial, and in three settings, namely, when

Uncorrected Proof

Table 3: Simulation results for the three profile models under different sample sizes and error variances.

Model	n	σ	C'''_{PPM}	Classic (OLS)			Bayesian (Gibbs)		
				$\hat{C}'''_{PPM}$	Bias	MSE	$\widehat{BC}'''_{PPM}$	Bias	MSE
$3+2x$	20	0.5	2.4718	2.5213	0.0495	0.0844	2.4663	-0.0055	0.0398
		0.8	1.5449	1.5311	-0.0137	0.0284	1.5219	-0.0229	0.0180
		1.0	1.2359	1.2399	0.0040	0.0207	1.2200	-0.0159	0.0115
	50	0.5	2.4906	2.4895	-0.0011	0.0314	2.4779	-0.0127	0.0132
		0.8	1.5566	1.5645	0.0079	0.0149	1.5519	-0.0047	0.0067
		1.0	1.2453	1.2535	0.0082	0.0092	1.2426	-0.0027	0.0042
	100	0.5	2.4969	2.5086	0.0116	0.0163	2.4972	0.0002	0.0076
		0.8	1.5606	1.5593	-0.0013	0.0058	1.5578	-0.0028	0.0037
		1.0	1.2485	1.2441	-0.0044	0.0032	1.2402	-0.0083	0.0020
$3.5+2x$	20	0.5	1.9946	2.0047	0.0100	0.0538	1.9983	0.0037	0.0360
		0.8	1.2467	1.2544	0.0077	0.0230	1.2269	-0.0198	0.0139
		1.0	0.9973	1.0115	0.0142	0.0165	0.9935	-0.0038	0.0103
	50	0.5	2.0100	2.0238	0.0139	0.0242	2.0251	0.0151	0.0134
		0.8	1.2562	1.2854	0.0292	0.0094	1.2653	0.0090	0.0055
		1.0	1.0050	1.0066	0.0017	0.0063	0.9969	-0.0081	0.0042
	100	0.5	2.0152	2.0168	0.0017	0.0127	2.0179	0.0027	0.0061
		0.8	1.2595	1.2616	0.0021	0.0047	1.2597	0.0003	0.0029
		1.0	1.0076	1.0110	0.0034	0.0036	1.0017	-0.0059	0.0021
$3.4+2.4x$	20	0.5	-4.1876	-4.3516	-0.1641	0.6204	-4.3544	-0.1668	0.4435
		0.8	-2.6172	-2.7708	-0.1535	0.4049	-2.8168	-0.1995	0.3992
		1.0	-2.0938	-2.2255	-0.1318	0.4002	-2.3046	-0.2109	0.4347
	50	0.5	-4.2167	-4.2257	-0.0091	0.2125	-4.2406	-0.0239	0.1643
		0.8	-2.6354	-2.7091	-0.0737	0.1886	-2.6957	-0.0603	0.1776
		1.0	-2.1083	-2.1872	-0.0788	0.1636	-2.2101	-0.1017	0.1684
	100	0.5	-4.2266	-4.2824	-0.0559	0.1097	-4.2734	-0.0469	0.0851
		0.8	-2.6416	-2.6764	-0.0348	0.0969	-2.6808	-0.0392	0.0811
		1.0	-2.1133	-2.1111	0.0021	0.0710	-2.1242	-0.0109	0.0685

the sample size is small (n = 20) and the error variance is high ($\sigma = 1.0$), the Bayesian estimator exhibits a slightly larger MSE than the classical method. This suggests that under extreme conditions of limited data and high noise, the flat priors may not provide sufficient stabilization, and the posterior inference becomes more sensitive to the observed data. Nevertheless, this limitation does not undermine the overall superiority of the Bayesian approach, as it remains highly effective in the vast majority of practical scenarios.

2. The bias of the Bayesian estimator is generally closer to zero than that of the classical estimator. This indicates that the Bayesian method not only provides more precise estimates (smaller MSE) but also maintains better accuracy (smaller absolute bias) across the evaluated scenarios.

3. The effect of sample size and error variance on estimation accuracy is clearly visible. As expected, for both estimators, the MSE decreases as the sample size increases, reflecting the greater amount of information available for estimation. The effect of the error variance is less straightforward, because the true value of the capability index itself depends on σ. As σ increases, the true capability index decreases in magnitude, and the absolute estimation errors therefore become smaller. Consequently, the MSE values are not directly comparable across different levels of σ, and the comparison of interest in this paper is between the two estimators within each σ level, rather than

Uncorrected Proof

across different σ levels.

To provide a visual summary of these findings, Figure 2 displays the MSE of both the classical and Bayesian estimators as a function of sample size for the three profile models. In each figure, the two estimators are distinguished by color, and the three error variance levels are distinguished by line type. The rate of decrease is most rapid when moving from $n = 20$ to $n = 50$, after which the improvement becomes more gradual. This pattern is consistent across all models and error variance levels, confirming the expected behavior of both estimators.

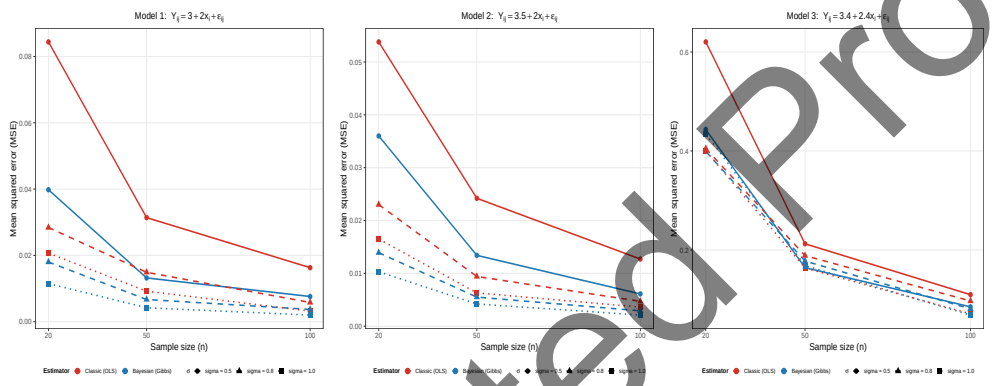

Figure 2: MSE comparison of the classical and Bayesian estimators across the three profile models.

4.4 Discussion

The simulation results clearly demonstrate the advantages of the proposed Bayesian index over its classical counterpart in simple linear profiles. The Bayesian estimator provides more accurate and precise estimates, especially in small-sample settings, where the classical estimator often suffers from large bias and high MSE. Notably, the non-informative priors employed here do not impose any regularization on the estimates; therefore, the observed superiority over the classical estimator stems from the Bayesian treatment of parameter uncertainty rather than from prior shrinkage.

It is important to note that the performance of the Bayesian estimator is not uniform across all models. For Model 3, which has a steeper slope and more extreme parameter values, this advantage is less pronounced, and in a few cases, the Bayesian estimator performs slightly worse than the classical method. This suggests that the choice of priors and the structure of the model may interact in complex ways, and that further research could explore the use of more informative priors or alternative parameterizations for such challenging settings.

This behavior can be attributed to three factors. First, with flat priors, the posterior mean of the regression coefficients is essentially equivalent to the OLS estimate, so the variance-reduction benefit of the Bayesian approach is minimal in this setting. Second, the capability index is a highly nonlinear function of the model parameters, and the posterior mean of a nonlinear function is not equal to the function of the posterior mean. For Model 3, where the true index is negative and large in magnitude, this nonlinearity is more pronounced and can introduce additional error. Third, when the

Uncorrected Proof

error variance is large, the likelihood becomes relatively flat, and the posterior distribution is dominated by the likelihood, with the MCMC sampling adding a small amount of Monte Carlo noise. These observations do not undermine the overall advantage of the Bayesian approach, but they do highlight the importance of prior specification in challenging settings and motivate the use of informative or shrinkage priors in future work.

It should be noted that the simulation study was conducted within the standard framework in which the capability index is defined, namely normally distributed, independent errors with constant variance. This framework provides a controlled setting for comparing the two estimators, but it does not cover situations in which the errors are non-normal, heteroscedastic, or serially dependent. Such departures may affect both the value of the index and the properties of its estimators, and their systematic investigation is left for future work.

In the three settings where the Bayesian estimator yields a larger MSE, the difference is small in absolute terms and is confined to the most challenging conditions, namely Model 3 with a small sample and a high error variance. These differences are therefore not practically meaningful and do not alter the overall conclusion that the Bayesian approach is preferable in the vast majority of practical scenarios.

Overall, the results of this simulation study provide strong empirical evidence in support of the Bayesian approach for capability assessment in simple linear profiles. The method is particularly recommended for practitioners who work with limited data or who require a more comprehensive quantification of uncertainty through credible intervals.

4.5 Sensitivity analysis to prior specification

The posterior estimates reported in the previous sections were obtained under the non-informative priors specified in Section 3. To examine whether the conclusions are sensitive to this choice, three alternative prior specifications were considered in addition to the main specification. The four specifications are summarized below.

- **A (main analysis):** a flat prior for the regression coefficients, $p(A_0, A_1) \propto 1$, and the Jeffreys prior for the error variance, $p(\sigma^2) \propto 1/\sigma^2$.
- **B:** proper but diffuse priors, with $\sigma^2 \sim \text{Inv-Gamma}(0.001, 0.001)$ and $A_0, A_1 \sim N(0, 1000)$.
- **C1:** $A_0, A_1 \sim N(0, 100)$ and a half-Cauchy prior on the error standard deviation, $\sigma \sim \text{Half-Cauchy}(0, 5)$.
- **C2:** the same as C1, but with the scale of the half-Cauchy prior set to one, $\sigma \sim \text{Half-Cauchy}(0, 1)$, so that the scale reflects the order of magnitude of the observed error standard deviation.

These specifications were chosen to span the range of prior beliefs commonly encountered in the Bayesian regression literature, from fully non-informative to weakly informative. Specification A represents the non-informative approach, specification B represents proper but diffuse priors that are widely used in practice, and specifications C1 and C2 follow the weakly informative recommendation of Gelman (2006), with two different scales for the half-Cauchy prior. Other proper priors, such as heavier-tailed or shrinkage priors, were not considered, because they are designed for different modelling purposes, such as variable selection or high-dimensional regression, and are

Uncorrected Proof

not expected to alter the conclusions in the present low-dimensional setting. The half-Cauchy prior was implemented through the auxiliary-variable representation of Makalic and Schmidt (2015), which preserves conjugacy and allows the Gibbs sampler of Section 3 to be used without modification. The choice of the half-Cauchy family follows the recommendation of Gelman (2006), who showed that the inverse-gamma prior can be unexpectedly informative near zero and advocated a half-Cauchy prior whose scale is chosen according to the scale of the data. For each specification, the Gibbs sampler was run for 10,000 iterations, with the first 5,000 discarded as burn-in, and the posterior distribution of the capability index was obtained by applying the procedure described in Section 3.4.

The results are presented in Table 4. Because the posterior distribution of the capability index is noticeably heavy-tailed, the posterior median and the 5% trimmed mean are reported as the primary summaries, together with the 95% credible interval. The heavy tail arises from the nonlinearity of the capability index and from the ratio structure of its denominator, and it makes the posterior mean and standard deviation less stable than the median and the trimmed mean.

Table 4: Posterior summaries of the capability index under four prior specifications for the calibration data.

Specification	Posterior median	5% trimmed mean	95% credible interval	Interval width
A	0.1905	0.1820	$[-0.1178, 0.3860]$	0.5037
B	0.1888	0.1792	$[-0.1493, 0.4205]$	0.5698
C1	0.1907	0.1801	$[-0.1166, 0.3848]$	0.5014
C2	0.1906	0.1813	$[-0.1286, 0.4006]$	0.5292

The four specifications lead to very similar conclusions. The posterior medians lie between 0.1888 and 0.1907, the trimmed means between 0.1792 and 0.1820, and all four credible intervals include zero and have comparable widths. The differences among the specifications are therefore small relative to the uncertainty reflected in the intervals, and the conclusions of the paper are not sensitive to the choice of prior. The results for specification C1 are particularly informative: although the posterior mean and standard deviation are affected by the heavy tail, the median, the trimmed mean, and the credible interval remain close to those obtained under the other specifications. This is consistent with the recommendation of Gelman (2006) that the scale of a half-Cauchy prior should be chosen according to the scale of the data; the scale of five is too large for the present data, whereas the scale of one in specification C2 leads to a posterior that is well behaved and in close agreement with specifications A and B.

Taken together, these results indicate that the posterior inference on the capability index is driven mainly by the data and is not materially affected by the prior specification. The non-informative priors used in the main analysis therefore provide a reasonable and objective basis for the conclusions of the paper, while the sensitivity analysis confirms that alternative proper and weakly informative priors lead to essentially the same assessment of process capability.

Uncorrected Proof

5 Application to real data

In this section, the practical applicability of the proposed Bayesian framework is illustrated using a dataset from a pressure gauge calibration process. The device measures pressure (in PSI) based on voltage output (in mV), and the relationship between these two variables is assumed to be linear.

The dataset was collected from a manufacturing plant over a period of 20 consecutive production days. For each day, one calibration run was performed at each of the four specified voltage levels. Prior to the capability assessment, the stability of the calibration process was verified by quality engineers using standard control charting techniques; however, this aspect is beyond the scope of the present study. The data analysed here are assumed to originate from a process that is in a state of statistical control, and the sole objective is to evaluate its inherent capability using the proposed index. A total of $n = 20$ independent calibration runs were conducted at each of $k = 4$ voltage levels: $x = 2, 4, 6$, and 8 mV. The specification limits were defined as $\pm 5\%$ of the target value at each level, i.e., $LSL_i = 0.95 \times T_i$ and $USL_i = 1.05 \times T_i$, where $T_i = 0.8 + 2.2x_i$ is the theoretical target line derived from the device's design specifications. The complete set of observed pressure values is presented in Table 5.

Table 5: Calibration data for the pressure measurement device.

Sample	$x = 2$	$x = 4$	$x = 6$	$x = 8$
1	5.5513	10.0257	13.9344	18.1279
2	5.5635	8.5092	14.3781	18.2343
3	5.0295	9.0484	13.9303	19.4904
4	5.4224	9.9121	13.5497	18.8901
5	4.6682	9.4011	14.6724	18.5792
6	5.6678	10.4735	13.6134	17.4681
7	4.2414	10.6831	13.7110	18.7722
8	5.5673	9.5026	14.4871	19.7181
9	6.4295	10.5795	14.1526	18.6947
10	5.0055	8.6028	15.0606	18.4155
11	5.8771	8.1718	13.3638	18.9623
12	5.7127	10.4764	13.1521	18.7404
13	5.5499	8.8159	13.6758	19.5686
14	5.2322	9.8110	13.5974	18.5668
15	5.6147	10.0943	15.2870	16.9918
16	5.2898	8.7945	14.3320	19.3540
17	4.8479	8.5006	14.5329	19.3561
18	5.5101	8.8226	14.0328	17.9292
19	4.5704	10.9983	14.8416	18.9656
20	5.6958	9.1131	14.2858	19.0128

A visual inspection of the data is provided in Figure 3, which displays the observed pressure values along with the fitted OLS line, the target line, and the specification limits. The fitted line, obtained as $\hat{Y} = 0.7648 + 2.2316X$, is almost perfectly superimposed on the target line ($Y = 0.8 + 2.2X$), indicating that the device operates with negligible systematic bias. The coefficient of determination ($R^2 = 0.9825$) further confirms the adequacy of the linear model.

Prior to the capability assessment, the stability of the process and the adequacy of the model assumptions were verified. The standard diagnostic plots are presented in Figure 4. The normal Q-Q plot of the standardized residuals follows a straight line, and

Uncorrected Proof

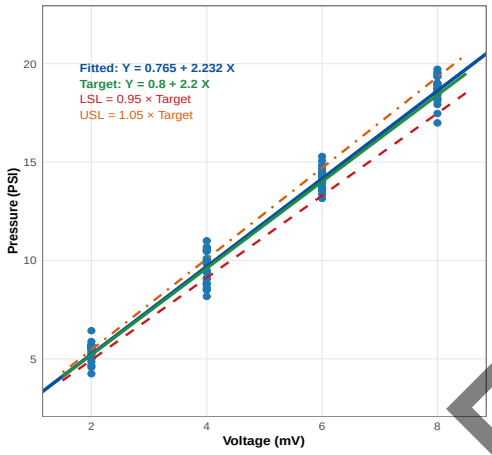

Figure 3: Calibration data with fitted line, target line, and specification limits.

the plot of residuals against fitted values shows no discernible pattern, supporting the assumptions of normality and constant variance. To verify statistical stability, a control chart was constructed for the residuals as presented in Figure 4. All residual values fall well within the 3σ control limits, and no systematic patterns are observed, confirming that the process was in a state of statistical control during the data collection period.

In addition to the visual diagnostics, formal goodness-of-fit tests were conducted. The Shapiro–Wilk test for normality of the residuals yielded a p-value of 0.3114, and the Breusch–Pagan test for constant variance yielded a p-value of 0.6878. Both p-values are considerably greater than the conventional significance level of 0.05, indicating that there is no statistical evidence to reject the model assumptions.

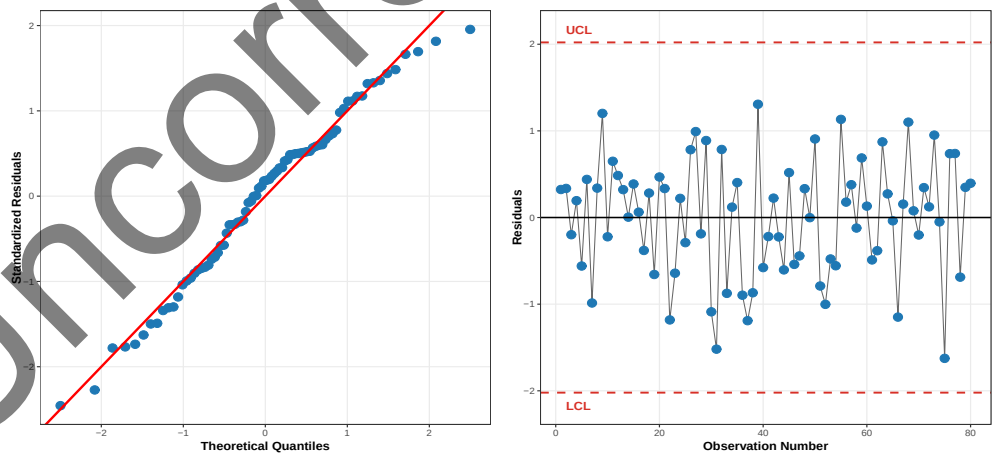

Figure 4: Model diagnostics: (a) normal Q-Q plot of the standardized residuals and (b) control chart for the standardized residuals.

To examine the performance across the voltage range, the local capability indices

Uncorrected Proof

$\hat{C}'''_{ppi}$ were computed at each level using the classical OLS method. These values were found to be $0.1112, 0.1805$, 0.2466, and 0.3090 for $x = 2, 4, 6$, and 8, respectively, showing a clear increasing trend as the voltage increases. This behavior is expected, as the specification limits become wider at higher voltage levels due to the fixed percentage definition. The overall classical estimate, obtained by averaging the local indices, is $\hat{C}'''_{ppM} = 0.2118$.

For the Bayesian approach, the point estimate of the overall capability index was obtained by averaging the index over the posterior draws, yielding $\widehat{BC}'''_{ppM} = 0.2053$, along with a 95% credible interval of $[-0.1348, 0.405]$. A summary of the parameter estimates and the capability indices for both methods is presented in Table 6.

Table 6: Comparison of classical and Bayesian estimates for the calibration example.

Parameter	Classic (OLS)	Bayesian (Gibbs)
Intercept (A_0)	0.7648	0.7673
Slope (A_1)	2.2316	2.2310
Error Variance (σ^2)	0.4539	0.4653
Capability Index (C_{ppM})	0.2118	0.2053
95% Uncertainty Interval	N/A	$[-0.1348, 0.405]$

The classical OLS method provides only a point estimate of 0.2118, without any quantification of its uncertainty. In contrast, the Bayesian approach gives a similar point estimate (0.2053) along with a 95% credible interval $[-0.1348, 0.405]$. The width of this interval reflects the limited sample size and the moderate variability in the data, both of which are naturally captured by the Bayesian framework.

Unlike the classical confidence interval, which is based on the hypothetical repetition of sampling and is often misinterpreted, the Bayesian credible interval has a direct probabilistic interpretation. Specifically, this interval means that, given the observed data and the assumed prior distributions, the probability that the true capability index lies within this range is 0.95. This intuitive interpretation is one of the key advantages of the Bayesian framework, as it allows quality engineers to make probabilistic statements about the process capability directly from the data. For the pressure gauge calibration example, the interval suggests that although the point estimate is positive, there is considerable uncertainty about the true capability, which should be taken into account when making decisions regarding process approval or corrective actions.

Notably, the capability index is not bounded below by zero, and negative values carry a clear practical meaning. Mathematically, a negative index arises when the fitted response at a given level falls outside the specification limits, which makes the numerator of the index negative. In practical terms, this indicates a process that is not merely incapable but is actually operating outside the acceptable limits, implying a high proportion of non-conforming items. In the present example, the negative lower bound of the credible interval reflects both the severe incapability of the calibration process and the substantial estimation uncertainty associated with the limited sample size. For quality engineers, such a result constitutes a clear signal that immediate corrective action is required before the process can be approved for production.

It is worth emphasizing that the fitted line overlaps the target line almost perfectly, indicating that the device is well-calibrated with negligible bias. However, the capability index remains low (0.21), which is primarily due to the relatively large variability

Uncorrected Proof

in the measurements ($\sigma \approx 0.68$). This example clearly demonstrates that a process can be accurate (centered on target) but still incapable if the variability is not adequately controlled. The Bayesian credible interval, by quantifying this uncertainty, provides a more complete picture of process performance and helps quality engineers distinguish between bias-related and variability-related issues.

Overall, this example demonstrates that the Bayesian framework provides a more informative assessment of process capability by explicitly quantifying estimation uncertainty, which is essential for reliable decision-making in quality engineering.

6 Conclusion

In this paper, a Bayesian framework was developed for profile capability index, denoted by BC'''_{ppM}, in the context of simple linear profiles. Non-informative priors were employed, and a Gibbs sampling algorithm was used to draw samples from the joint posterior distribution of the profile parameters, from which the posterior distribution of the index was derived. In contrast to the classical approach, the proposed method provides not only point estimates but also credible intervals, enabling a more comprehensive quantification of estimation uncertainty. An extensive simulation study was conducted to compare the performance of the proposed Bayesian estimator with that of the classical ordinary least squares estimator under various process conditions. The results consistently demonstrated that the new index, when estimated using the Bayesian framework, outperforms its classical counterpart in terms of both bias and mean squared error across the majority of settings, yielding particularly notable advantages in small-sample scenarios. The method also exhibited greater stability across different levels of error variance, making it a reliable tool for quality engineers. Although these performance gains were less pronounced for steeper profiles under extreme noise and very small samples, this does not undermine the overall superiority of the proposed Bayesian approach. For future work, several extensions can be considered. Alternative prior specifications, such as informative or shrinkage priors, could be investigated to further enhance performance in challenging settings. The proposed framework could also be extended to non-linear or multivariate profiles, and the incorporation of autocorrelation or fuzzy specification limits would increase its practical relevance, as would an assessment of robustness to non-normal errors and heteroscedasticity. Additionally, the development of user-friendly software would facilitate its adoption by practitioners. Overall, the proposed Bayesian framework provides a reliable, flexible, and uncertainty-aware tool for estimating the capability index BC'''_{ppM} in simple linear profiles, and is expected to be particularly valuable in applications where sample sizes are limited or where a thorough understanding of estimation uncertainty is essential.

Uncorrected Proof

Acknowledgement

The author would like to sincerely thank the Editor and the anonymous reviewers for their careful review, insightful comments, and constructive suggestions, which significantly improved the quality and clarity of this manuscript .

References

Abbasi Ganji, Z. (2025). Fuzzy-based functional capability indices for simple linear profile, *Journal of Mahani Mathematical Research*, **14**(2):373–402.

Abbasi Ganji, Z. and Sadeghpour Gildeh, B. (2016). A class of process capability indices for asymmetric tolerances. *Quality Engineering*, **28**(4):441–454.

Abbasi Ganji, Z. and Sadeghpour Gildeh, B. (2020). Fuzzy process capability indices for simple linear profile. *Journal of Applied Statistics*, **47**(12):2136–2158.

Abbasi Ganji, Z. and Sadeghpour Gildeh, B. (2023). A new process capability index for simple linear profile. *Communications in Statistics-Theory and Methods*, **52**(11):3879–3894.

Adibfar, S. and Noorossana, R. (2024). Process Capability Analysis for Simple Linear Profiles in Multistage Processes. *Pakistan Journal of Statistics and Operation Research*, **20**(1):139–155.

Adibfar, S., Noorossana, R. and Ahmadi, O. (2023). Process capability analysis for multivariate simple linear profiles in a multistage process. *Journal of Industrial and Systems Engineering*, **14**(4):158–173.

Ebadi, M. and Shahriari, H. (2013). A process capability index for simple linear profile. *International Journal of Advanced Manufacturing Technology*, **64**(5):857–865.

Gelman, A. (2006). Prior distributions for variance parameters in hierarchical models (comment on article by Browne and Draper), *Bayesian Analysis*, **1**(3): 515-534.

Gelman, A., Carlin, J.B., Stern, H.S. and Rubin, D.B. (1995). *Bayesian Data Analysis*, Chapman and Hall/CRC.

Gelman, A. and Rubin, D.B. (1992). Inference from iterative simulation using multiple sequences. *Statistical science*, **7**(4):457–472.

Hosseinifard, S.Z. and Abbasi, B. (2012a). Evaluation of process capability indices of linear profiles. *International Journal of Quality & Reliability Management*, **29**(2):161–176.

Hosseinifard, S.Z. and Abbasi, B. (2012b). Process capability analysis in non normal linear regression profiles. *Communication in Statistics-Simulation and Computation*, **41**(10):1761–1784.

Kang, L. and Albin, S.L. (2000). On-line monitoring when the process yields a linear profile. *Journal of Quality Technology*, **32**(4):418–426.

Kim, K., Mahmoud, M.A. and Woodall W.H. (2003). On the monitoring of linear profiles. *Journal of Quality Technology*, **35**(3):317–328.

Makalic, E. and Schmidt, D.F. (2015). A simple sampler for the horseshoe estimator. *IEEE Signal Processing Letters*, **23**(1):179–182.

Uncorrected Proof

Noorossana, R., Saghaei, A. and Amiri, A. (2011). *Statistical Analysis of Profile Monitoring*. John Wiley & Sons.

Pakzad, A., Razavi, H. and Sadeghpour Gildeh, B. (2021). Functional process capability indices for a simple linear profile in fuzzy environment. *Journal of Industrial and Systems Engineering*, **13**(4):1–22.

Pakzad, A., Razavi, H. and Sadeghpour Gildeh, B. (2022). Developing loss-based functional process capability indices for simple linear profile. *Journal of Statistical Computation and Simulation*, **92**(1):115–144.

Pakzad, A., Yeganeh, A., Noorossana, R. and Shongwe, S.C. (2024). Process Capability Index for Simple Linear Profile in the Presence of Within-and Between-Profile Autocorrelation. *Mathematics*, **12**(16):2549.

Plummer, M., Best, N., Cowles, K. and Vines, K. (2006). CODA: convergence diagnosis and output analysis for MCMC. *R News*, **6**(1):7–11.

R Core Team (2024). *R: A Language and Environment for Statistical Computing*. R Foundation for Statistical Computing, Vienna, Austria.

Shahriari, H. and Sarrafian, M. (2009). Assessment of process capability in linear profiles. *Proceedings of the 6th International Industrial Engineering Conference*, Tehran, Iran.

Wang, F.K. (2014a). A process yield for simple linear profiles. *Quality Engineering*, **26**:311–318.

Wang, F.K. (2014b). Measuring the process yield for simple linear profiles with one-sided specification. *Quality and Reliability Engineering International*, **30**(8):1145–1151.

Woodall, W.H. (2007). Current research on profile monitoring. *Production*, **17**:420–425.

Wu, X.F. (2015). An assessment approach for process capability in simple linear profile, In: Qi, E., Shen, J. and Dou, R. (eds). *Proceedings of the 22nd International Conference on Industrial Engineering and Engineering Management*, pp. 613–620, Paris: Atlantis Press.

Zou, C., Zhang, Y. and Wang, Z. (2006). Control chart based on change-point model for monitoring linear profiles. *IIE Transactions*, **38**(12):1093–1103.

Uncorrected Proof